*Original Research*

# Electrochemical Properties and Pollution Remediation Mechanism of P-MFC Anode under Cadmium Stress

**Yan Yang\*, Qianyong Shen**

College of Environment and Safety Engineering, Chang Zhou University, Changzhou, China

## Abstract

To explore the remediation feasibility of heavy metal pollution in wetland soil using a plant-microbial fuel cell (P-MFC) and the corresponding mechanism, a P-MFC system was constructed with in situ simulations of real wetland environment. By using *Typhalatifolia* L. as the trial plant, the electrochemical properties of the anode under different cadmium (Cd) concentrations are analyzed by cyclic voltammetry and electrochemical impedance, and the microbial community structure is determined by high-throughput sequencing. The maximum P-MFC output voltage of 546.65 mV and Cd accumulation of 36.461 mg/kg at the *Typhalatifolia* L. roots are revealed. Cd stress could not only decrease the output voltage and anodic electrochemical activity of the P-MFC system but also affect the accumulation ability of *Typhalatifolia* L. and the internal resistance and microbial community structure of P-MFC. We find it feasible to apply P-MFC to large-scale heavy metal remediation in wetland soil, but it is critical to consider the tolerance range of pollution stress to achieve the best balance between energy output and environmental restoration.

**Keywords**: soil moisture content, remote sensing retrieval, sensitive spectral band

## Introduction

Plant microbial fuel cells (P-MFC) are a type of microbial fuel cell (MFC) system where plants are involved and their rhizosphere secretions are directly used as microbial electron donors after photosynthesis [1]. Microbes with electricity production capability are enriched at the anode, degrading the organic substances which are secreted by plant roots, and transporting the generated electrons to the anode and then the cathode through an external circuit load, thus providing sustainable renewable energy [2].

There have been a few studies on electricity production from P-MFC through biodegradation, electrode redox reactions, and plant hyperaccumulation for environmental remediation, environmental management technology, and energy engineering technology, indicating a good perspective [3, 4]. Among these studies, Wetser et al. inoculated P-MFC with aerobic wastewater, utilized three layers of graphite felt stack at the anode and achieved an average power density of 240 mW/m² plant growth area [5]. By adding ferricyanide to reduce the cathode resistance in the cathode chamber, an average current density of

\*e-mail: yy129129@163.com

83 mA/m² plant growth area and an average output voltage of 214 mV were obtained [6]. Moqsud et al. built the P-MFC system by composting and using carbon fiber electrode materials, resulting in a maximum output voltage of 700 mV [7]. Lu et al. [8] modified the cathode of the P-MFC system by using an activated carbon catalyst to obtain a maximum current density of 105 mA/m². In the field of environmental pollution control, P-MFC is used in water pollution control [9], artificial wetland coupling treatment environment [10], and so on. However, the existing work focuses on indoor or laboratory conditions, although achieving high performance, it may not be practical for large-scale applications.

China has a wetland area of 53.6026 million hectares, accounting for about 10% of the world's wetland area, ranking first in Asia and fourth in the world. The development of a P-MFC natural metabolic pollution purification system based on in situ simulations of the real environment will have great potential in application prospects. In recent years, the wetland soil pollution in China is becoming more and more serious, and 25% of wetland pollution is highly severe and difficult to control (http://www.shidi.org/). The evaluation of wetland pollution reveals that the heavy metal Cd generally has an excessive content, serving as one of the main pollutants in wetland soil.

In this study, a real wetland environment is simulated and the P-MFC system is constructed using *Typhalatifolia* L. as the trial plant, which is a wetland marsh plant widely distributed in Asia, Oceania and other regions, to explore the electricity production performance of P-MFC under different Cd concertations and the effects of hyperaccumulation and transfer of Cd in *Typhalatifolia* L.The mechanism of electricity production and environmental remediation of the P-MFC is studied by analyzing the microbial community structure through anodic electrochemical performance test and high-throughput sequencing analysis, aimed at providing a theoretical basis for scale application of P-MFC in wetland and feasibility study of electricity production and soil pollution remediation.

## Material and Methods

### Construction of the P-MFC System

The P-MFC was constructed by using *Typhalatifolia* L., a perennial Mongolian herb. The schematic diagram of P-MFC is shown in Fig. 1, composed of a single-chamber structure with graphite felt as the electrode material. The lower layer was the anode anaerobic region buried in the soil, and the upper aqueous phase was the cathode aerobic region suspended in the soil and water interface. The anode and the cathode were connected by wires and loaded with an external resistance of 1000 Ω. The sample soil was obtained from the wetland park at Changzhou City, Jiangsu Province, containing 31.27%
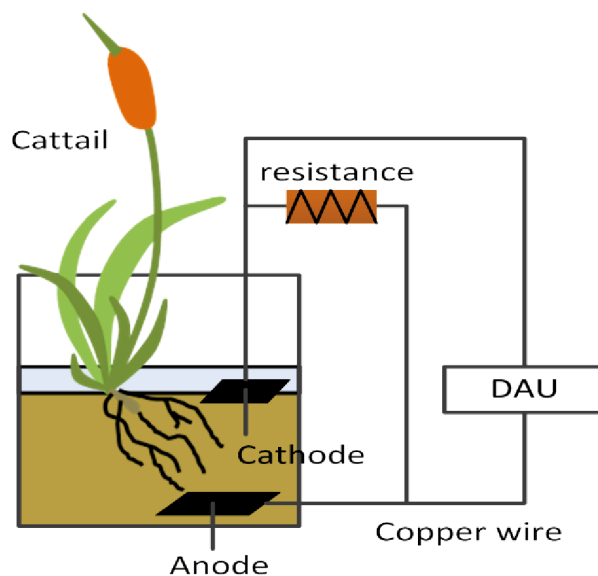


Fig. 1. A schematic diagram of the P-MFC device.

of moisture, 0.62% of salt, 17.52 g/kg of organic matter, 2.98 g/kg of total nitrogen, 98.6 mg/kg of available potassium, 40.26 mg/kg of available phosphorus and no Cd. The size of the experimental device was $\Phi 15 \times 30$ cm, with an anode area of 125 cm² and cathode area of 100 cm² per the pre-experiment. The soil was exposed to the $CdCl_2 \cdot 2.5H_2O$ solution to accumulate Cd. According to the Soil Environmental Quality Standard (GB 15618-2008), soil samples with Cd concentrations of 0, 1, 5, 10 and 30 mg/kg were obtained and denoted as $T_0$, $T_1$, $T_5$, $T_{10}$, and $T_{30}$, respectively. The original solid sample without *Typhalatifolia* L. planting was treated as the control sample T. Three *Typhalatifolia* L. were planted in each soil sample inside a box and cultured in a greenhouse during an appropriate planting time (June to September 2016), with ambient humidity of about 50% RH. *Typhalatifolia* L. growth was regularly supplemented with deionized water.

### Analysis and Testing

The output voltage was monitored using an Agilent data collector (Agilent 34970A).

Electrochemical Impedance Spectroscopy (EIS) analysis was performed on an electrochemistry workstation (CHI660E) to characterize the internal resistance of P-MFC. The EIS test conditions were as follows: the initial voltage of 0 V (vs. SCE), AC amplitude of 10 mV, and frequency range of 0.1-10 MHz. The equivalent circuit was fitted by utilizing Zview. The electrochemical performance of the anode was measured by cyclic voltammetry (CV) in a three-electrode configuration. The bio-anode of the P-MFC was used as the working electrode and the cathode in the reactor as the counter electrode. The saturated calomel electrode was used as the reference electrode. The CV test was carried out at a scanning
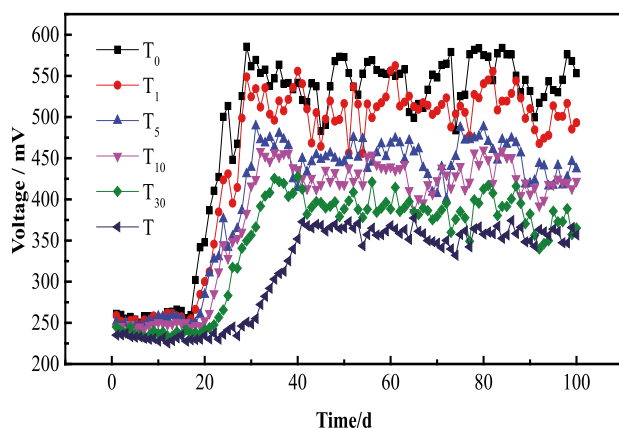
Fig. 2. The daily average output voltage of P-MFC under different cadmium exposure concentrations.

rate of 10 mV $s^{-1}$ with a potential window of -0.8 to 0.6 V.

The anode graphite felt was rinsed with deionized water to remove residual particles and then the anodic biofilm was collected using a sterile blade for testing.

16S primers: forward primer 515F (5'-GTGCCAGCMGCCGCGGTAA-3') and reverse primer 907R (5'-CCGTCAATTCMTTTRAGTTT-3') (Guangzhou Meige Biotechnology Co., Ltd.); Premix Taq, 100bp DNA ladder, λ-HindIII Marker, and DL 2000 DNA Marker (TaKaRa); agarose (Guangzhou Haoma Biotechnology Co., Ltd.).

DNA extraction kit and MiSeq pe250 high-throughput sequencer (MOBIO, USA); QuantoniT Broad-Range DNA Detection Kit (Invitrogen, USA); Next Ultra II DNA Library Kit (NEB, USA); E.Z.N.A Gel Recovery Kit (OMEGA, USA); S1000PCR Instrument (BioRad, USA).

PCR amplification: 6 μL of 10x Ex Taq buffer, 6 μL of dNTP, 0.6 μL of BSA, 0.3 μL of Ex Taq, 1 μL of DNA, 1.2 μL of forward primer, and 1.2 μl of reverse primer, diluted to 60 μL with water.

PCR amplification conditions: pre-denaturation at 94ºC for 5min; denaturation at 94ºC for 30s and annealing at 52ºC for 30s; extension at 72ºC for 45s and amplification for 31 cycles; extension at 72ºC for 10 min. The amplified product was obtained and identified by 1% agarose gel electrophoresis, and the gel was recovered using a gel recovery kit. The biomedical analysis was performed by high-throughput sequencing at Guangzhou Meige Biotechnology Co., Ltd.

## Results and Discussion

### Analysis of Electricity Production Capacity

MFC generally output voltage in three stages: delay, rising and stable stages [11]. The voltage outputs from 6 sets of MFC are shown in Fig. 2. While other conditions are consistent with the case, the start time and the output voltage are proportional to the Cd exposure concentration, indicating a long start time and a low output voltage of the MFC at a high Cd exposure concentration. The photosynthesis of carbon from higher plants can be released into the soil through the form of root exudates, providing nutrition and energy for the rhizosphere micro environment, producing microbes, and generating persistent electrons [12, 13]. However, Cd stress destroys the chloroplast bilayer structure of plant leaves, disintegrates the basal stacks, decreases the chlorophyll content, inhibits the photosynthetic efficiency of plants, and reduces the microbial activity in plant rhizosphere soil [14]. In this study, $T_1$ has the shortest start time and reaches the stable stage on the 29th day with a stable output voltage of 512.07 mV, while $T_5$, $T_{10}$, and $T_{30}$ are stabilized on the 30th, 31th, and 35th days, with stable output voltages of 451.52, 429.47, and 389.07 mV, respectively, compared with $T_0$, which is stabilized on the 29th day outputting a voltage of 546.65 mV. This fully demonstrates that Cd stress could affect the electricity production capacity of P-MFC. Yadav et al. [10] constructed a wetland-based microbial fuel cell (CW-MFC) for dye wastewater treatment and found that with the increase of dye wastewater concentration, electricity production performance decreased. Wang et al. [15] found that the addition of nitrate contaminates reduced the corresponding output voltage of MFC and prolonged the start period. This is consistent with our findings in this study that pollution stress will affect the electricity production capacity of P-MFC. De et al. constructed a rice-MFC and found

Table 1. The transfer and accumulation of Cd under different concentrations in *Typha latifolia* L.

| P-MFC | Initial Cd (mg/kg) | Shoots (mg/kg) | Roots (mg/kg) | Transfer Factor* | Bioaccumulation Factor* | |
|---|---|---|---|---|---|---|
| | | | | | Shoots | Roots |
| $T_1$ | 0.837 | 0.482 | 5.375 | 0.090 | 0.576 | 6.422 |
| $T_5$ | 4.050 | 0.647 | 9.532 | 0.068 | 0.160 | 2.354 |
| $T_{10}$ | 8.368 | 1.153 | 21.822 | 0.057 | 0.138 | 2.608 |
| $T_{30}$ | 24.439 | 2.857 | 36.461 | 0.078 | 0.117 | 1.492 |

*The Transfer Factor refers to the ratio of cadmium content in the shoots to the cadmium content in the roots; The Bioaccumulation Factor is to the ratio of cadmium content in the shoots/roots to the cadmium content in the soil.

that the MFC with plant had an electricity production efficiency of 0.1 W/m², which was about 7 times that of the plant-free MFC [16]. Liu et al. [17] planted water spinach in an artificial wetland environment, and the electricity production efficiency of MFC increased 142% to 12.42 mW/m². In this study, the start time of T is 12 days longer than that of $T_0$, and its stable output voltage is 36.31% lower, indicating that to a certain extent, the involvement of plants can promote the electricity production capacity of MFC.

In recent years, a number of research groups around the world have worked hard to improve electricity output of P-MFC from the initially reported efficiency of 6 to 390 mW/m² [18-20]. It is worth noting that the high electricity production efficiency of P-MFC has been achieved only in laboratory conditions or through microbial inoculation [21]. *In situ* wetland simulation of this study may not produce the best performance, but it is the only way to explore the large-scale application of P-MFC.

## Accumulation and Transfer of Cd in *Typhalatifolia* L.

It has been reported that a variety of hyperaccumulators accumulate Cd in root organs when remediating Cd-contaminated soil [22, 23]. Table 2 shows that at the end of the experiment, more heavy metal is found to have accumulated in roots than shoots of $T_1$, $T_5$, $T_{10}$, and $T_{30}$. When Cd enters the plant, it will combine with pectinate, protein and other substances to form a ligand, reducing the transfer of Cd ions through the membrane. The cell wall is the first barrier to prevent Cd ions from entering the plant cell, making the root cell wall a major site for Cd accumulation [24]. The increase of Cd concentration is negatively correlated with the bioaccumulation factor (BF) of Cd and output voltage. At a Cd concentration of 1 mg/kg, the BF and output voltage achieve the highest. When the Cd stress increases from 5 to 10 mg/kg, the change of BF is not obvious, and the stable output voltages are much lower than that of $T_1$. When the Cd concentration rises to 30 mg/kg, the plant is close to the tolerance threshold, and the BF decreases significantly and the output voltage

Table 2. Impedance values of P-MFC obtained by fitting the equivalent circuit.

| P-MFC | $R_s / \Omega$ | $R_{ct} / \Omega$ | $W / \Omega$ |
|-------|------|-------|--------------|
| $T_0$ | 5.73 | 51.29 | $4.78 \times 10^{-3}$ |
| $T_1$ | 4.49 | 48.22 | $6.93 \times 10^{-3}$ |
| $T_5$ | 4.53 | 33.99 | $7.58 \times 10^{-3}$ |
| $T_{10}$ | 4.98 | 34.68 | $7.73 \times 10^{-3}$ |
| $T_{30}$ | 6.33 | 98.95 | $2.45 \times 10^{-3}$ |
| T | 6.28 | 71.55 | $5.83 \times 10^{-3}$ |

is the lowest. It is known that the first step in the entry of metal ions into the plant is root absorption, which is the first rate-limiting step for hyperaccumulators [25]. It has been reported that the root activity of *Typhalatifolia* L. is closely related to Cd concentration. With the increase of Cd concentration, the toxic effect gradually increases, leading to the decrease of root activity [26], so the high Cd concentration will result in low BFs of plants.

Morari et al. constructed an artificial wetland system with *Typhalatifolia* L. to carry out urban sewage treatment. The removal rates of various heavy metals such as Al, Cu, and Cd were 31-96% and the BF of Cd was 1.62 mg/kg [27]. Chen et al. achieved a Cr removal rate of up to 87% via the water culture of *Typhalatifolia* L. [28]. Through the hydroponic system under greenhouse conditions, Pilonsmitsfound that the accumulation of Cd increased under the influence of Ca and Fe, achieving a Cd adsorption rate of up to 71% from a nutrient solution, and it mainly occurred in the roots [29]. Many studies have proven that *Typhalatifolia* L. is a type of hyperaccumulator that can remediate heavy metal pollution, but the study of *Typhalatifolia* L. incorporated with P-MFC for soil pollution remediation is rarely reported.

## Analysis of Anodic Electrochemical Performance

For P-MFC running under anaerobic conditions, electricigens consume organic matter at the anode to obtain the energy required to sustain the growth of the microorganism and produce electrons. The electrons reach the cathode through the external circuit to form the current loop [21]. The microbial transmission of electrons at the anode is the key step to achieving energy conversion [2], therefore, through the cyclic voltammetry and electrochemical impedance test of the anode, we can understand the microbial activity and internal resistance of P-MFC.

### Cyclic Voltammetry

Cyclic voltammetry (CV) can be used to characterize the electrochemical activity of microbes [30] or determine whether there is an electron shuttle or electron mediator produced by microorganisms in the system for electron transfer [31].

Fig. 3 shows that there are obvious redox peaks in the CV curves of $T_0$, $T_1$, $T_5$, $T_{10}$, and $T_{30}$ at a scan rate of 10 mV/s, indicating that microbes are present in the anode of the P-MFC under different pollution stresses [32]. The intensity of the peak represents the ability of the microbes to generate and transfer electrons. The oxidation peaks of $T_0$, $T_1$, $T_5$, and $T_{10}$ are located at about 0.1 V, while the oxidation peak of $T_{30}$ shifts to 0 V. Both $T_0$ and $T_1$ have reduction peaks at -0.4 V, and their oxidation peaks are located at a similar position, suggesting that their anode microbes have similar characteristics of electricity production. Two reduction

Fig. 3. CV curves of P-MFC anodes under different Cd concentrations.



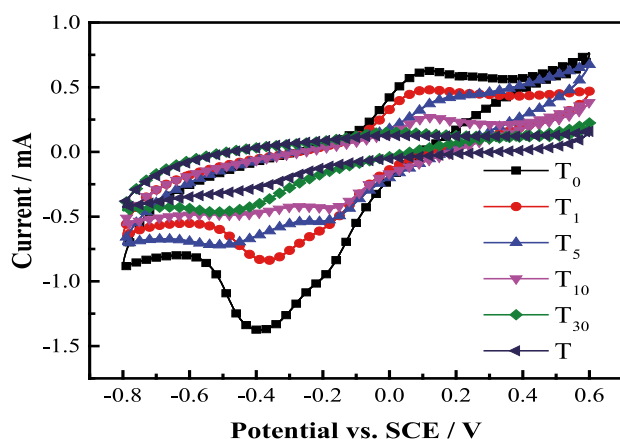Fig. 5. Nyquist plots of P-MFC at different Cd concentrations.

peaks are found at -0.2 and -0.5 V on the CV curve of $T_5$ and $T_{10}$, and only one reduction peak can be identified at -0.5 V for $T_{30}$.

$T_0$ has the largest anodic and cathodic peak current and the highest intensity of redox peaks among all P-MFC, indicating the strongest microbial electrochemical redox reactions with the highest redox activity. Peak intensity decreases with the degree of Cd pollution, as the electrochemical activity of P-MFC anodes is inhibited, which is consistent with the trend of electricity production capability of P-MFC under different concentrations of Cd stress. It is probably because, with the increase of Cd concentration, the toxic effect of heavy metals on microbes becomes significant enough to affect the electrochemical activity of microbes in the anode, leading to the decrease of electricity production capacity.

T has no obvious oxidation peak, but a reduction peak appearing at -0.5 V with the lowest peak intensity. It is clear from the above discussion that without the growth of *Typhalatifolia* L., no root exudates are available to nurture the microbial at the anode, resulting in a weak microbial activity to inhibit electricity production, and thus the lowest output voltage.

## Electrochemical Impedance Analysis of the Anode Biofilm

To study the composition and change of the internal resistance of the P-MFC system under different Cd concentrations, the electrochemical impedance spectroscopy (EIS) test is carried out when the output voltage is stable. On the complex impedance plane, the
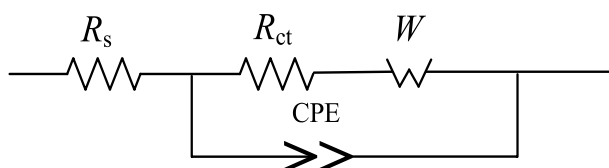


Fig. 4. The equivalent circuit of P-MFC at different Cd concentrations.
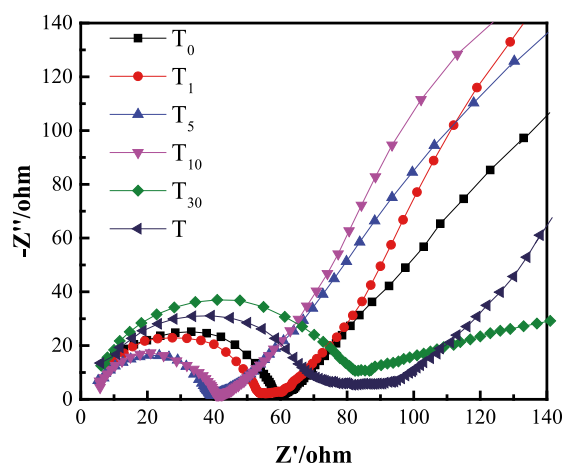
real part (Z') and the absolute value of the imaginary part (-Z'') of the measured impedance are taken as the abscissa and the ordinate to plot the Nyquist diagram. The EIS test results at different Cd concentrations are shown in Fig. 5. The alternating current impedance diagram is simulated with Zview, and the equivalent circuit is shown in Fig. 4. The electric double layer between the electrode and the solution is generally expressed by the equivalent capacitance. In practice, since the carbon felt has unevenness and is attached with a biofilm, a "diffusion effect" is generated so that the double layer resistance is represented by a constant-phase angle element CPE. $R_s$ is the ohmic internal resistance, and $R_{ct}$ is the internal resistance of the charge, which reflects the characteristics of the activation process. $W$ is the diffusion impedance (Warburg Impedance), representing the characteristics of the mass transfer process [33].

Table 2 shows the impedance values of P-MFC obtained by fitting the equivalent circuit. For $T_0$, $T_1$, and $T_5$, their $R_{ct}$ accounts for 89.94%, 91.47%, and 88.22%, respectively, of the total impedance, indicating that the electrochemical reactions of the anode biofilm are controlled by the charge transfer process. It can also be seen that $R_{ct}$ of $T_1$ and $T_5$ decreases by 5.99% and 33.73% compared to $T_0$. This suggests that when Cd stress is lower than 5 mg/kg, the increase of the stress leads to the decrease of $R_{ct}$, and the activation energy barrier of microbial catalytic reactions is lowered. It is very likely that an appropriate amount of heavy metal ions are deposited to modify graphite felt and improve the anode performance so that the electron diffusion is enhanced, thus reducing $R_{ct}$ [34]. Furthermore, $R_{ct}$ of $T_{10}$ increases slightly, while $R_{ct}$ of $T_{30}$ increases sharply, achieving 1.93 times of that of $T_0$. We believe that at a very high concentration, the toxic effects of heavy metals on the anodic microbes are significant, and they inhibit the microbial activity and affect the electron transfer process [35]. Therefore, the internal resistance of the anode rises sharply and the output voltage of P-MFC is dramatically reduced.

$R_{ct}$ of T is 91.12% of the total resistance and 1.40 times that of $T_0$. This makes clear that the growth of *Typhalatifolia* L. can improve the anode performance to generate a much higher output voltage. Therefore, in the practical application of P-MFC to remediate Cd-contaminated media, it is necessary to pay special attention to the pollutant concentration and the tolerance threshold of hyperaccumulators to achieve high removal efficiency and energy recovery efficiency.

## Analysis of the Anode Microbial Community Structure

The microbial community plays an important role in the process of electron transfer to the electrode and the degradation of the pollutants. To analyze the changes of P-MFC microbial community structure under different Cd concentrations, the anodes of $T_0$, $T_1$, $T_5$, $T_{10}$, and $T_{30}$ are sampled for high-throughput sequencing analysis, and the results are shown in Fig. 6. In this study, the microbes of P-MFC are originated from the *in-situ* wetland soil.

Fig. 6a shows the relative abundance of the microbes on the phylum level. The microbial community in all five samples mainly consists of 11 phylums, including Proteobacteria, Bacteroidetes, Actinobacteria, Acidobacteria, Chloroflexi, Firmicutes, Spirochaetes, Planctomycetes, Verrucomicrobia, Crenarchaeota, and Euryarchaeota.

Among them, Proteobacteria is the most dominant species in the anode of all five P-MFC with a relative abundance range of 21.19-42.85%. With the increase of Cd concentration, the relative abundance of Proteobacteria first increases and then decreases, and it reaches the highest value of 42.85% in $T_5$, but drops to the lowest value of 21.19% in $T_{30}$. It is demonstrated that the charge transfer resistance of the anode increases with the increase of Cd concentration up to 5 mg/kg ($T_5$). It has been reported that most of the electricigens are derived from Proteobacteria [36], and the abundance of Proteobacteria may affect the internal resistance of P-MFC, where a high relative abundance of *Proteobacteria* leads to a low internal resistance. Bacteroidetes is the second most dominant species with a relative abundance range of 11.15% (in $T_0$) to 20.21% (in $T_5$). Among the rest of the phylum species, the relative abundance of Actinobacteria and Chloroflexi (3.43-18.79%) are relatively high, and they reach the highest values of 18.79% and 18.15% in $T_0$ and $T_5$, respectively. The relative abundance of Acidobacteria and Firmicutes are low, with only 2.27-6.71% and 1.78-5.44%, respectively. However, they are also electricigens with low electricity production capacity [37-39]. In $T_{30}$, the microbial community structure is drastically changed, and the relative abundance of Euryarchaeota increases from 0.29-2.42% (in $T_0$, $T_1$, $T_5$ and $T_{10}$) to 29.43% (in $T_{30}$), making Euryarchaeota the most dominant species in the anode.
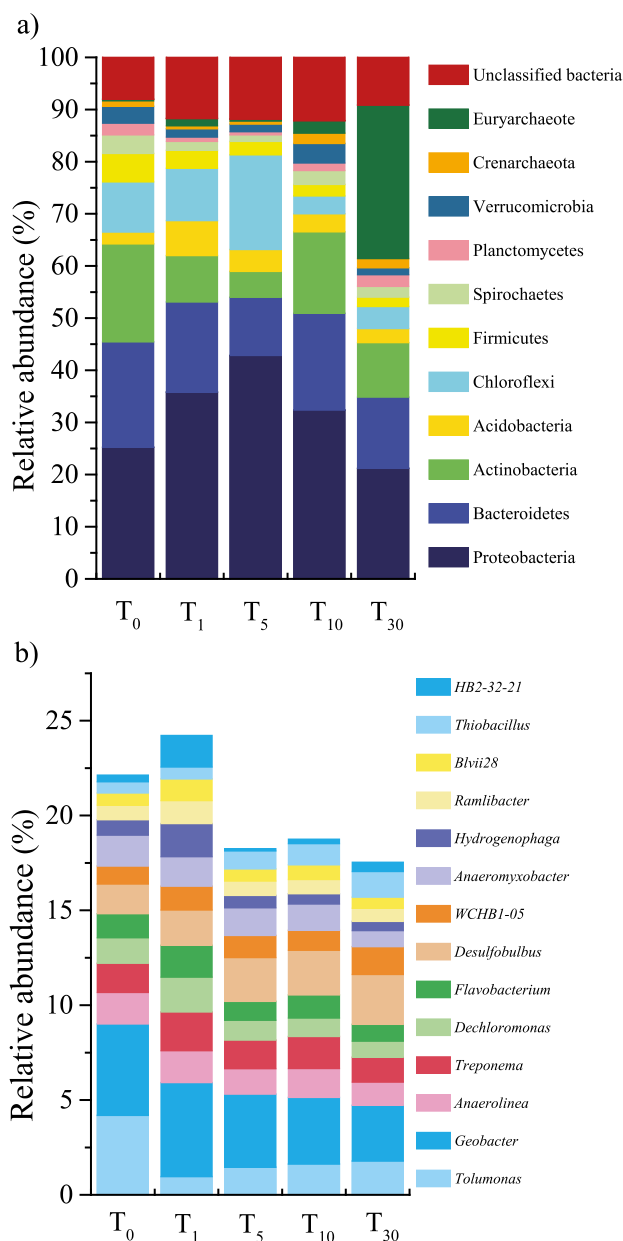


Fig. 6. The composition of anodic biofilm community under different Cd concentrations on the level of a) phylum and b) genus.

On the level of the genus, the microbial community in all five samples mainly consists of 14 genera, including *Tolumonas*, *Geobacter*, *Anaerolinea*, *Treponema*, *Dechloromonas*, *Flavobacterium*, *Desulfobulbus*, WCHB1-05, *Anaeromyxobacter*, *Hydrogenophaga*, *Ramlibacter*, *Blvii28*, *Thiobacillus*, and HB2-32-21. Among all P-MFC, *Geobacter* is the most dominant species, and its relative abundance decreases with the increase of Cd concentration and accounts for 2.94% in $T_{30}$ and 4.96% in $T_1$. *Geobacter* belongs to Proteobacteria and is the main electricigen in the anode microbial community [40], widely distributed in the Fe(III) reduction environment, such as freshwater sediments and groundwater sediments with organic or heavy metal pollution, with an important bioremediation

function. Combined with the output voltage and CV curves, it is shown that with the increase of Cd concentration, the change of electricigens abundance in the anode affects the electrochemical activity, which further impacts the output voltage of P-MFC. In $T_0$, *Tolumonas* is the second most dominant species with a relative abundance of 4.19%, and it plays an important role in nitrogen fixation, plant growth promotion, and degradation of pollutants [41]. The relative abundance of *Tolumonas* in P-MFC first decreases and then increases with the increase of Cd concentration, with the lowest value of 0.96% in $T_1$. *Desulfobulbus* being the second most dominant species among all P-MFC, and its relative abundance accounts for 1.56-2.63% and shows an upward trend with the increase of Cd concentration.

From the microbial community structure under different Cd stress, it is known that the abundance changes of the electricigens Proteobacteria on the phylum level and *Geobacter* on the genus level are consistent with the changes of the internal resistance of the P-MFC and electrochemical activity as characterized from CV, respectively. This proves that with the increase of Cd concentration, the microbial community structure change affects the electrochemical activity and internal resistance, thus the output voltage.

## Conclusions

The feasibility of P-MFC scale application in a wetland area is studied by the simulation of the real wetland environment and the evaluation of the electricity production and environmental remediation function of *Typhalatifolia* L. under different Cd stress. We find that the output voltage of P-MFC with initial Cd exposure ($T_1$, $T_5$, $T_{10}$, and $T_{30}$) decreases with the increase of Cd stress and is lower than that of the pollution-free $T_0$; while all P-MFC with *Typhalatifolia* L. growth output higher voltages over T, the plant-free MFC. The BF is low under the high concentration of Cd pollution, and the accumulation of Cd is significant in the roots, suggesting that *Typhalatifolia* L. is the optimal trail plant.The electrochemical properties and microbial community structure of P-MFC are analyzed to explore the electricity production and remediation mechanism. Proteobacteria, on the phylum level, and *Geobacter*, on the genus level, are the most dominant electricigens and they account for 21.19-42.85% and 2.94-4.96% of the microbial community. *Geobacter* is an internationally recognized pollution-degrading microbe, which to a certain extent ensures normal operation of the P-MFC in the wetland environment. However, with the increase of Cd stress, the number of electricigens decreases, as well as electrochemical activity. This indicates that Cd stress changes the electricity production capacity of the P-MFC system by affecting the number and activity of electricigens. Furthermore, when the number of electricigens in the anode decreases, the BF is also reduced and the effect of Cd poisoning, instead of the anode modification, becomes more serious, inhibiting the function of the P-MFC and making the environmental remediation ineffective. In the future study for large-scale application of P-MFC, the tolerance threshold for plants and microbial communities need to be fully considered.

## Conflict of Interest

The authors declare no conflict of interest.

## References

1. NITISORAVUT R., REGMI R. Plant microbial fuel cells: A promising biosystems engineering. Renew SustEnerg Rev. **76**, 81, **2017**.
2. TANG X.T., Du Z.W., Li H.R. Anodic electron shuttle mechanism based on 1-hydroxy-4-aminoan thraquinone in microbial fuel cells. ElectrochemCommun. **12**, 1140, **2010**.
3. XU M.Y., WU W.M., WU L.Y., HE Z.L., NOSTRAND J.D.V., DENG Y., LUO J., CARLEY J., GINDER-VOGEL M., GENTRY T.J., GU B., WATSON D., JARDINE P.M., MARSH T.L., TIEDJE J.M.,HAZEN T., CRIDDLE C.S., ZHOU J.Z. Responses of microbial community functional structures to pilot-scale uranium in situ bioremediation. ISME J. **4**, 1060, **2010**.
4. YAN Z.S., SONG N., CAI H.Y., TAY J.H., JIANG H. Enhanced degradation of phenanthrene and pyrene in freshwater sediments by combined employment of sediment microbial fuel cell and amorphous ferric hydroxide. J Hazard Mater. **199-200**, 217, **2012**.
5. WETSER K., SUDIRJO E., BUISMAN C.J.N., STRIK D.P.B.T.B. Electricity generation by a plant microbial fuel cell with an integrated oxygen reducing biocathode. ApplEnerg. **137**, 151, **2015**.
6. WETSER K., LIU J., BUISMAN C., STRIK D. Plant microbial fuel cell applied in wetlands: Spatial, temporal and potential electricity generation of Spartinaanglica, salt marshes and Phragmitesaustralis, peat soils. Biomass Bioenerg. **83**, 543, **2015**.
7. MOQSUD M.A., YOSHITAKE J., BUSHRA Q.S., HYODO M., OMINE K., STRIK D. Compost in plant microbial fuel cell for bioelectricity generation. Waste Manage. **36**, 63, **2015**.
8. LU L., XING D., REN Z.J. Microbial community structure accompanied with electricity production in a constructed wetland plant microbial fuel cell. Bioresource Technol. **195**, 115, **2015**.
9. MATHURIYA A.S., BAJPAI S.S., GIRI S. Epipremnumaureum (money plant) as cathode candidate in microbial fuel cell treating domestic wastewater. J Biochem Tech. **6**, 1025, **2015**.

10. YADAV A.K., DASH P., MOHANTY A., ABBASSI R., MISHRA B.K. Performance assessment of innovative constructed wetland-microbial fuel cell for electricity production and dye removal. Ecol Eng. **47**, 126, **2012**.

11. AELTERMAN P., FREGUIA S., KELLER J., VERSTRAETE W., RABAEY K. The anode potential regulates bacterial activity in microbial fuel cells. Appl Microbiol Biot. **78**, 409, **2008**.

12. HE J., ZHANG S., TENG J.Q., XIA S.B. Progress on application of aquatic plants in microbial fuel cells. Environ Sci Technol. **2013**, 100, **2013**.

13. RONALD P.C., SHIRASU K. Front-runners in plant-microbe interactions. Curr Op in Plant Biol. **15**, 345, **2012**.

14. TENG Y., WANG X., LI L., LI Z., LUO Y. Rhizobia and their bio-partners as novel drivers for functional remediation in contaminated soils. Front Plant Sci. **6**, 32, **2015**.

15. WANG R.C., ZHOU X.Y., YAO J.B., LI X.L. Influence of nitrate concentration in anolyte on electricity generation of microbial fuel cell. Acta Sci Vet. **36**, 1608, **2016**.

16. DE S.L., VAN den B.L., DANG H.S., HÖFTE M., BOON N., RABAEY K., VERSTRAETE W. Microbial fuel cells generating electricity from rhizodeposits of rice plants. Environ Sci Technol. **42**, 3053, **2008**.

17. LIU S.T., SONG H.L., LI X.N., YANG F. Power Generation Enhancement by Utilizing Plant Photosynthate in Microbial Fuel Cell Coupled Constructed Wetland System. Int J Photoenergy. **2013**, 15158, **2013**.

18. HELDER M., STRIK D.P., HAMELERS H.V., KUIJKEN R.C., BUISMAN C.J. New plant-growth medium for increased power output of the Plant-Microbial Fuel Cell. Bioresour Technol. **104**, 417, **2012**.

19. HELDER M., STRIK D.P., TIMMERS R.A. Resilience of roof-top Plant-Microbial Fuel Cells during Dutch winter. Biomass Bioenerg. **51**, 1, **2013**.

20. TIMMERS R.A., ROTHBALLER M., STRIK D.P., ENGEL M., SCHULZ S., SCHLOTER M., HARTMANN A., HAMELERS B., BUISMAN C. Microbial community structure elucidates performance of Glyceria maxima plant microbial fuel cell. Appl Microbiol Biot. **94**, 537, **2012**.

21. KARTHIKEYAN R., WANG B., XUAN J., WONG J.W.C., LEE P.K.H., LEUNG M.K.H. Interfacial electron transfer and bioelectrocatalysis of carbonized plant material as effective anode of microbial fuel cell. Electrochim Acta. **157**, 314, **2015**.

22. SCHICKLER H., CASPI H. Response of antioxidative enzymes to nickel and cadmium stress in hyperaccumulator plants of the genus Alyssum. Physiol Plantarum **105**, 39, **2010**.

23. LIN Y.F., AARTS M.G. The molecular mechanism of zinc and cadmium stress response in plants. Cell Mol Life Sci. **69**, 3187, **2012**.

24. SARRET G., SAUMITOU-LAPRADE P., BERT V., PROUX O., HAZEMANN J.L., TRAVERSE A., MARCUS M.A., MANCEAU A. Forms of zinc accumulated in the hyperaccumulator Arabidopsis halleri. Plant Physiol. **130**, 1815, **2002**.

25. LASAT M.M., PENCE N.S., GARVIN D.F., EBBS S.D., KOCHIAN L.V. Molecular physiology of zinc transport in the Zn hyperaccumulator Thlaspi caerulescens. J Exp Bot. **51**, 71, **2000**.

26. LYUBENOVA L., SCHRÖDER P. Plants for waste water treatment-Effects of heavy metals on the detoxification

system of *Typha latifolia*. Bioresource Technol. **102**, 996, **2011**.

27. MORARI F., FERRO N.D., COCCO E. Municipal Wastewater Treatment with *Phragmites australis*, L. and *Typha latifolia*, L. for Irrigation Reuse. Boron and Heavy Metals. Water Air Soil Poll. **226**, 1, **2015**.

28. CHEN Y.L., HONG X.Q., HE H., LUO H.W., QIAN T.T., LI R.Z., JIANG H., YU H.Q. Biosorption of Cr (VI) by Typha angustifolia: mechanism and responses to heavy metal stress. Bioresource Technol. **160**, 89, **2014**.

29. PILONSMITS E. Increased accumulation of cadmium and lead under Ca and Fe deficiency in *Typha latifolia*: A study of two pore channel (TPC1) gene responses. Environ Exp Bot. **115**, 38, **2015**.

30. NIESSEN J., SCHRÖDER U., ROSENBAUM M., SCHOLZ F. Fluorinated polyanilines as superior materials for electrocatalytic anodes in bacterial fuel cells. Electrochem Commun. **6**, 571, **2004**.

31. BABAUTA J., RENSLOW R., LEWANDOWSKI Z., BEYENAL H. Electrochemically active biofilms: facts and fiction. A review. Biofouling. **28**, 789, **2012**.

32. YOON S.M., CHOI C.H., KIM M., HYUN M.S., SHIN S.H., YI D.H., KIM H.J. Enrichment of electrochemically active bacteria using a three-electrode electrochemical cell. J Microbiol Biotechnol. **17**, 110, **2007**.

33. ZHAO S.L., LI Y.C., YIN H.J., LIU Z.Z., LUAN E.X., ZHAO F., TANG Z.Y., LIU S.Q. Three-dimensional graphene/Pt nanoparticle composites as freestanding anode for enhancing performance of microbial fuel cells. Sci Adv. **1**, e1500372, **2015**.

34. LOWY D.A., TENDER L.M., ZEIKUS J.G., PARK D.H., LOVLEY D.R. Harvesting energy from the marine sediment-water interface II: Kinetic activity of anode materials. Biosens Bioelectron. **21**, 2058, **2006**.

35. SONG T.S., JIN Y., BAO J., KANG D., XIE J. Graphene/biofilm composites for enhancement of hexavalent chromium reduction and electricity production in a biocathode microbial fuel cell. J Hazard Mater. **317**, 73, **2016**.

36. CHAUDHURI S.K., LOVLEY D.R. Electricity generation by direct oxidation of glucose in mediator less microbial fuel cells. Nat Biotechnol. **21**, 1229, **2003**.

37. BOND D.R., LOVLEY D.R. Evidence for involvement of an electron shuttle in electricity generation by Geothrix fermentans. Appl Environ Microb. **71**, 2186, **2005**.

38. NIESSEN J., SCHRÖDER U., SCHOLZ F. Exploiting complex carbohydrates for microbial electricity generation – a bacterial fuel cell operating on starch. Electrochem Commun. **6**, 955, **2004**.

39. ZHANG YF, MIN BK, HUANG LP, ANGELIDAKI I. Generation of Electricity and Analysis of Microbial Communities in Wheat Straw Biomass-Powered Microbial Fuel Cells. Appl Environ Microbiol. **75**, 3389, **2009**.

40. BOND D.R., HOLMES D.E., TENDER L.M., LOVLEY D.R. Electrode-reducing microorganisms that harvest energy from marine sediments. Science. **295**, 483, **2002**.

41. LI Y.H., LIU Q.F., LIU Y., ZHU J.N., ZHANG Q. Endophytic bacterial diversity in roots of Typha angustifolia L. in the constructed Beijing Cuihu Wetland (China). Res Microbiol. **162**, 124, **2011**.